Journal of Ovonic Research Vol. 16, No. 5, September - October 2020, p. 309 - 321

SCHOTTKY DIODE FABRICATION VIA COLD SUBSTRATE EVAPORATED Ag ON SOL-GEL DERIVED ZnO ULTRA-THIN FILMS FOR SEMICONDUCTOR DEVICES

E. F. KESKENLER [a,b*], M.HAİDAR [c]
[a]*Department of Electrical-Electronics Engineering, Faculty of Engineering and Architecture, Recep Tayyip Erdoğan University, Rize, Turkey*
[b]*Department of Advanced Technologies, Graduate School of Natural and Applied Sciences, Recep Tayyip Erdoğan University, Rize, Turkey*
[c]*Department of Energy Systems Engineering, Graduate School of Natural and Applied Sciences, Recep Tayyip Erdoğan University, Rize, Turkey*

ZnO thin films were grown on glass and SnO_2 substrate by using Sol-gel method with a simple, low cost-temperature and high controlled away. ZnO thin films were contacted with Ag in two different temperatures at 200K (cold substrate) and 300K (room temperature) by PVD Cold Substrate Method. Characterization of the obtained films and Schottky diodes studied by XRD, SEM, Optical and Electrical measurements. The average particle size and film thickness of the films were calculated as ~25 and ~300nm. Bandgap of the ZnO films coated on different substrates was calculated to be around 3.29-3.31 eV. Peaks of various types of defects were observed in different wavelengths from photoluminescence measurements. The barrier height and ideal factor values of Ag/ZnO Schottky diodes at 200K and 300K were (0.48-0.43eV; 15.60) and (0.66-0.15eV; 8.6-7.41), respectively. The series resistance values (4.46Ω; 4.88Ω) at 200K and (3.65Ω; 4.78Ω) at 300K were obtained from two different methods, respectively. Diodes made at 200K temperature were found to have a higher ideality factor. However, while 75% of all produced Schottky diodes at 200K substrate temperature show rectifying feature, this rate is only 25% in contacts made at 300K substrate temperature.

(Received July 17, 2020; Accepted October 15, 2020)

Keywords: Ag/ZnO, Diode, Cold substrate method, PVD, Sol-gel

1. Introduction

Thin films, electronic devices, and solar plates, which have gained great importance among recent research and development, form the basis of production technology. For this reason, many techniques have been developed in the production of thin films. Sol-gel method is one of the methods widely used in coating thin films by dip-coating or spin-coating techniques of nanostructured ceramic colloidal materials.

Sol-gel method is a process that can control various film parameters and has simple and low-cost features. It is significantly differentiated among other methods used in this context. Briefly, the Sol-gel process can be described as the formation of an oxide network through the polymer reactions of the molecules in the prepared liquid. The left is a solution containing colloidal particles or polymers that do not dissolve and settle in the solvent. These particles expand in solution and form a three-dimensional network. Sol-gel method can be used in many fields to prepare materials of various shapes and properties, such as the synthesis of porous structures, fine fibers, dense powders and thin films [1-4].

Zinc oxide (ZnO) is a unique material-substrate with semiconductor and piezoelectric properties. Nanostructured ZnO materials attract attention as they show superior performance in electronic, optical and photovoltaic applications [5, 6]. Zinc oxide is a compound semiconductor from the group II-VI in the periodic table, having a wide bandwidth of 3.37 eV. It has a high

* Corresponding author: keskenler@gmail.com

exciton binding energy of 60meV at room temperature [7]. Thin film ZnO semiconductor devices are attracted attention due to their superior performance in electronic, optical, and photonic applications. It is a cheap material that is non-toxic and can be found in various nanostructures, it has gained great importance in the field of technology due to these features. Short-wave nanolasers, very sensitive nanoscale gas sensors, field-effect transistors, transducers, nanoresonators, (electrical circuit containing capacitors, inductors and producing electrical oscillations), nano support arms, optoelectronic devices, field emissions (on phones using) and nano support arms (nanorobot) as a basic material for applications of ZnO [8, 9].

Ohmic and Schottky contacts are necessary to occurring the intended architecture of ZnO-based semiconductors with several electrical parameters. Improve the high-quality and suitable ohmic and rectifying contacts to achieve maximum efficiency is required for semiconductor devices. Fabrication of an intended quality rectifying contact on n-type ZnO crystal is harder because of high donor concentration at the surface field coming from defects such as oxygen vacancies (V_o) or zinc interstitials (Zn_i) or both [10-12] which affect the barrier height of metal-semiconductor.

The metal diffusion into semiconductors, the defects in the surface area, critical process temperature and vacuum level for optimizing contact are several acknowledged problems of blocking the formation of Schottky contacts. Cold Substrate Method is a novel, current and appropriate technique that enables the contact of semiconductor materials at low temperatures [13]. For these reasons, Cold Substrate Method can be used to minimize the activation energy of the atoms on the surface to improve the contact quality.

In this study, the sol-gel method was used to deposit ZnO thin films on the SnO_2 substrate due to advantages such as saving, low expense and temperature, and applicability of its experimental procedure with large area production [14]. Although Ag has been widely used for Schottky barriers on II-VI semiconductors, according to our knowledge only several studies [15-17], about Ag contact onto Sol-gel derived ZnO diode have been reported and there is no any study about Ag contacting via Cold Substrate Method on sol-gel deposited ZnO for Ag/ZnO device. The device performance of the Ag/n-ZnO/SnO_2 has been reported with characteristic properties of ZnO thin films on glass and SnO_2 substrate.

2. Experimental

In this study, glass and SnO_2 on glass were used as a substrate to deposit films. The substrates are cleaned from the dirty particles affecting the film. Pure and clean substrates were obtained by waiting for up to 5 minutes using ethanol compound, then adding 5 minutes in drinkable non-ionic water and cleaning it for 10 minutes by putting it on an ultrasonic device. This procedure was repeated twice. The substrates were dried under 350K after cleaning. Zinc Acetate Dihydrate [$Zn(CH_3COO)_2 \bullet H_2O$] with the molecular weight 219.49g / mol, was taken as the starting materials to prepare the solution. 5 ml of 2-Methoxyethanol and Monoethanolamine (MEA) with the molecular weight 61.08g/mol were used as solvent and stabilizer, respectively. 0.4M ZnO solution was prepared. 0.439 g Zinc Acetate salt and 0.112g Monoetanolamine were calculated and added to the pre-solution. After preparing the solution, it was stirred at 323K for 2 hours to allow the formation of colloidal particles in the magnetic stirrer and solution gelation. The transparent solution color turned brown at the end of the process. In order to form ZnO thin film layer with spin coating Sol-gel Method, the coating process was carried out in the air environment by rotating 2500 revolutions per minute (rpm) on the glass and SnO_2 substrate for 20 seconds. The coated films were then sintered for drying at 473K for 5 minutes. These operations were repeated as 7 cycles in order to reach a certain film thickness. An important point for device applications that the ZnO thin films were not annealed. Low-temperature applications for production-line is significant for environmental processes and low-cost. The crystal structure and surface morphology of the films were examined in detail with the help of XRD and SEM devices. The optical properties of the films were measured with a UV optical spectrometer. Electrical properties were determined with the help of a complex multimeter (Keithley 2400 Model).

After examining the structural, morphological, optical and electrical properties of the ZnO films, Schottky diodes in Ag/ZnO/SnO_2/Glass architecture were obtained by evaporating Ag at 200K temperature and also 300K (normal room conditions) on ZnO films. The heater which converts the material into saturated steam consists of the material to be evaporated, the section with the holders of the substrate and the adjustable window, the heater to adjust the substrate temperature, the copper pipe where the liquid nitrogen will circulate to cool the substrate, the vacuum chamber, the mechanical pump and the vacuum pump are the basic features and components of the Cold Substrate Physical Vapor Deposition System (CS-PVD) (Patented Vaksis PVD handy/1DLE-LN). In the system, Ag coating was carried out for 7 minutes by determining the substrate temperature at 200K and 300K, the pressure of the vacuum medium 1.5×10^{-5} - 8×10^{-6} torr and the applied current value 33A. Schottky contacts onto ZnO/SnO_2 films were fabricated by evaporating Ag with a mask and 20 Schottky diodes around 1.5 mm in diameter for each temperature value were obtained.

3. Results and discussion

X-ray diffraction results of ZnO thin films grown on SnO_2 and glass substrate are presented in Fig. 1. It has been determined from the graph that XRD peaks of ZnO belong to (002), (100), and (101) planes at 2θ angles 31.8°, 34.4° and 36.3°, respectively. There is no dominant peak in the crystal structure deposited on the glass substrate, however, (002) peak is the dominant peak for the deposited ZnO film on the SnO_2 substrate. The change in intensity of plane orientations may be related to the crystal structure of the SnO_2 substrate. The intensity of the resulting peaks is low, and a gauss effect is observed. This can be explained by the obtained films containing nanoparticles. Again, it can influence that the film layers being very thin. From the XRD results, it was determined that the ZnO structure was in the wurtzite hexagonal structure. Since ZnO films are not grown on a special cubic substrate and are not produced under high pressure (10Gpa), this may influence this situation. According to Rajput et al.[18], similar results were found in which the ZnO structure obtained from the X-ray diffraction device (002) had a preferentially oriented wurtzite hexagonal crystal structure. The average crystal size of the ZnO film was calculated by using the Scherrer equation utilized form X-ray diffraction line-broadening;

$$D = \frac{0.94\lambda}{\beta \cos\theta} \tag{1}$$

where D is grain size, β is broadening of diffraction line obtained at half of its maximum intensity in radians unit, θ is Bragg angle and λ is wavelength of X-rays. The crystal size of sample was calculated from the (002) peak. The calculated size of the ZnO crystallite is 25 nm (± 0.05 nm). The lattice parameter c of a unit cell of crystal was calculated from the following relation;

$$\frac{1}{d^2} = \frac{4}{3}\left(\frac{h^2 + hk + k^2}{a^2}\right) + \frac{l^2}{c^2} \tag{2}$$

where d is an interplanar distance of atomic planes obtained from nλ=2dSinθ as 2.60 Å and (*hkl*) is Miller indices.

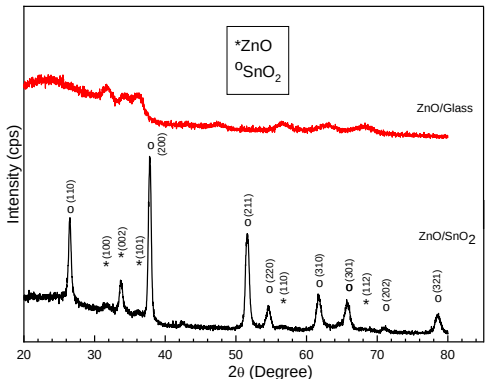

Fig. 1. X-ray diffraction spectra of the ZnO thin films on glass and SnO_2 substrates.

$$a = \frac{\lambda}{\sqrt{3}\sin\theta(100)} \tag{3}$$

$$c = \frac{\lambda}{\sin\theta(002)} \tag{4}$$

The lattice constants, determined from the 2θ values of (002) and (100) diffraction peaks and found by substituting in the equations (3) and (4), were c = 5.30 Å (± 0.005 Å) and a = 3.18 Å (± 0.005 Å). According to a similar study by Keskenler et al. [19], very close values were reported for the crystal grain size, lattice parameters and crystal structure of ZnO thin films.

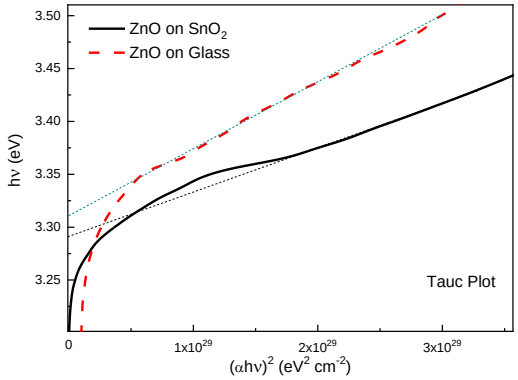

Fig. 2. (hυ) versus $(\alpha h\upsilon)^2$ graph (Tauc Plot) of ZnO thin films on glass and SnO_2 substrates relation with the bandgap energy of films.

The semiconductor bandgap can be calculated from the absorption coefficient and the relationship between photon energy. The absorption coefficient from the Beer Lambert equation (5) is expressed as follows [20];

$$T = (1 - R)e^{-\alpha d} \tag{5}$$

Here, T is transmittance, R is reflectance, is absorption coefficient and d is the film thickness obtained from cross-sectional SEM images. Photon energy (hυ) versus $(\alpha h\upsilon)^2$ graph is presented of the films in Figure 2. The point where the linear parts of the graph curves intersect the (hυ) axis for the value $(\alpha h\upsilon)^2 = 0$ are bandgap energy (E_g) values. This method is known as the Tauc method and is expressed by equation (6).

$$\alpha^2 \propto \left(h\upsilon - E_g\right) \tag{6}$$

As mentioned, the energy difference between the transmission band in the crystal and the valence band is known as the Bandgap energy. It is an important parameter that characterizes conductors, insulators, and semiconductors. This energy difference for semiconductors ranges from approximately 0.5 to 5eV. While the bandgap energy values for transparent oxide semiconductors are around 3-5eV, these values may vary depending on the concentrations, types, coating method and ambient conditions of the compounds in the solution to be prepared. Energy band gap values of ZnO films deposited on SnO_2 and glass substrate were found to be around 3.29 and 3.31 eV. Results consistent with the values obtained by [21].

It is a powerful technique to investigate separate energy levels with photoluminescence (PL) optical stimulation and extract valuable information about semiconductor sample composition, quantum well thickness, or quantum dot monodispersity. In this technique, the electron, which is stimulated to the transmission band, descends into the valence band and merges with the space and creates a photon at the frequency equivalent to the energy it loses. Photoluminescence is affected by the properties of the material, defects in crystalline and optical stimulation parameters [22-24]. The PL spectra are shown in Figure 3. Three peaks occurred in the PL spectra of ZnO on glass and SnO_2 substrate. The peak of the strong emission locked at about 376 and 388nm in the UV region originated from the recombination of free excitons in the near-band-edge of ZnO. The other peaks (at 535-541nm and 609-627nm) which exhibited a broad emission at the green band was commonly originated from various defects or impurities, such as the ionized oxygen vacancies and interstitial zinc atoms [34,35].

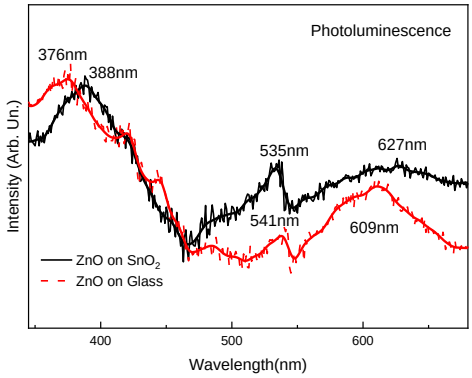

Fig. 3. Photoluminescence spectra of the ZnO thin films on glass and SnO2 substrates.

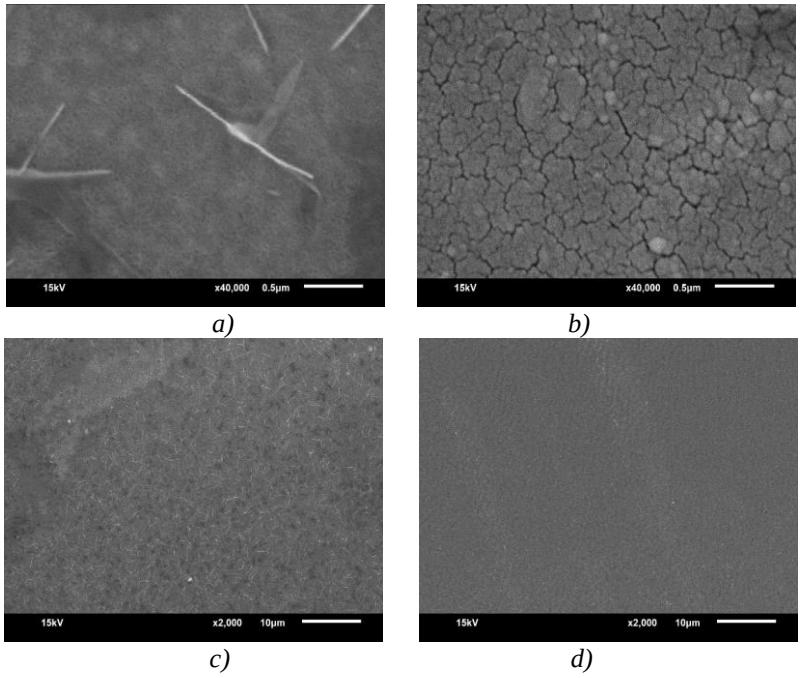

Fig. 4. SEM images of ZnO samples on SnO_2 and glass substrates. a) ZnO on SnO2 substrate with 0.5 micron scale magnification, b) ZnO on glass with 0.5 micron scale magnification, c) ZnO on SnO2 substrate with 10 micron scale magnification and d) ZnO on glass with 10 micron scale magnification.

Scanning Electron Microscope (SEM) images of the films are given in Figure 4. It is clearly seen from the images that the morphological features of the films vary according to the substrate. In Figures 4-a and -c, it is seen that the film is grown on Tin Oxide (SnO_2) substrate, whereas the needle-like structures caused by thin folds appear, but the structure is smaller in size. It is clear that the films obtained on the glass (Figures 4-b and -d) exhibit larger particle structures compared to the samples grown on the SnO_2 substrate. The separation regions of the film grains contain wide valley pores. When moving away from the films together with the figures 4-c and d, it is observed that the homogeneous needle-like structures of the ZnO sample, which enlarged on the SnO_2 substrate, became clear, while a wavy structure formed on the surface of the sample grown on the glass substrate. It can be concluded that this is caused by the surface interactions of the atomic layers first attached to the base. It is seen that Figure 4-a is tighter and more homogeneous than 4-b and Figure 4-b is in a fragmented structure. The reason for this situation can be explained as the fact that the ZnO crystal has been grown on the SnO_2 semiconductor substrate and this structure provides ZnO with reference mold growth and a stronger adhesion to the surface. Film thicknesses can be seen from the cross-section SEM images presented in Figure 5. From the microscope images, film thicknesses were determined as average 320 nm for ZnO/SnO_2 sample and 149 nm for ZnO/Glass sample. It is understood from the images that the film thicknesses are homogeneous. In Figure 6, SEM images of Ag Schottky contacts made at 200K and 300K temperatures are given to ZnO structures grown on the SnO_2 substrate. The analysis of the surface morphologies and grain sizes of the films grown on the cold substrate (200K) and the substrate at room temperature (300K) were made with the help of Figure 6. It is clear that the Ag contact evaporated on ZnO at 200K temperature has much smaller grain sizes than those at 300K temperature. Ag film layer formed on a 200K temperature substrate has a smoother and non-porous structure than the other. It has Ag valley shaped pores on the substrate with 300K temperature and the grain sizes separated by these pores are quite large. Ag atoms evaporated in the vacuum ring are directed to the target substrate with their high energy and cause accumulation by hitting the target base. When the target substrate temperature is lowered, Ag atoms encounter a substrate with reduced surface activation energy. This situation shocks the Ag

atoms reaching the substrate with high energy and allows them to freeze on the ground. Thus, it enables more homogeneous and especially nano-sized small granular surface formations. It is concluded that the surface thermal energy of the target substrate has important effects on the metal contact to be coated. In Figure 6-c and d, the size of the contact area covered for both substrate temperatures is approximately 1.5mm^2.

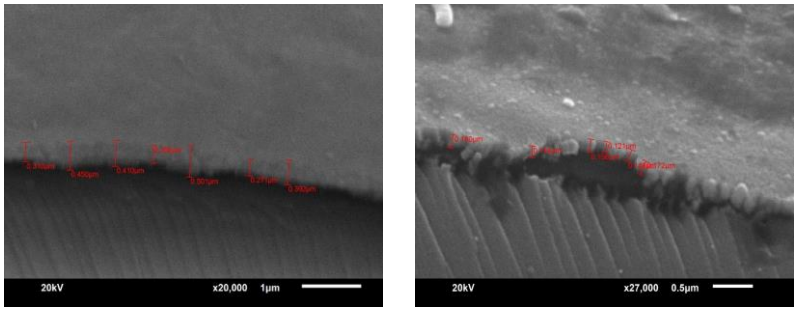

a) *b)*

Fig. 5. Cross-section SEM images of ZnO samples on SnO_2 and glass substrates for thickness.

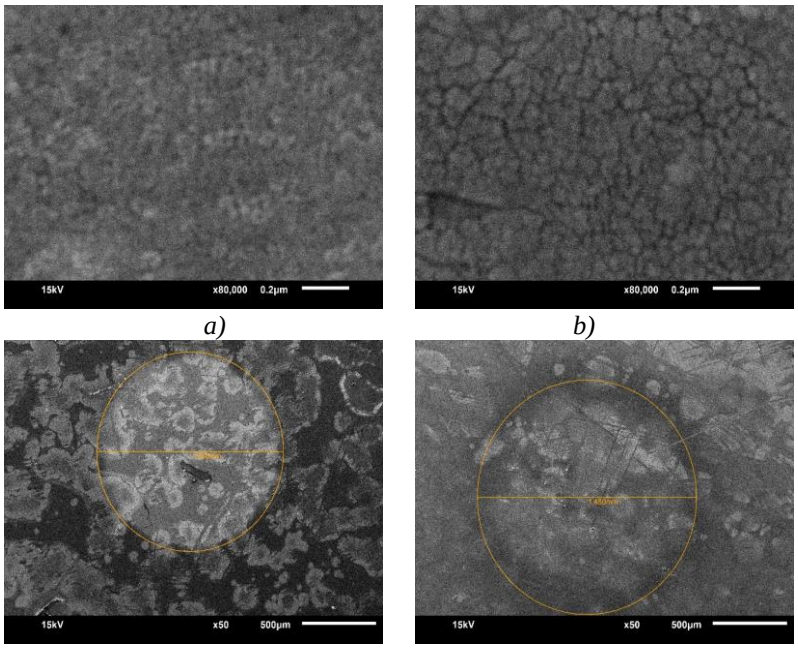

a) *b)*

c) *d)*

Fig. 6. SEM images of Schottky contacts of Ag on ZnO films at 200K and 300K that demonstrated differences between room and cold substrate temperature.

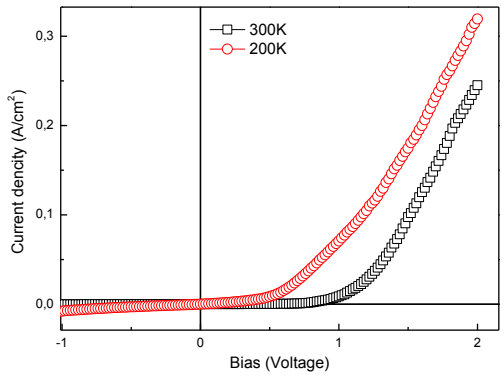

Fig. 7. Nonlinear current density-voltage (J-V) measurement curve of Ag/n-ZnO/ Schottky diode.

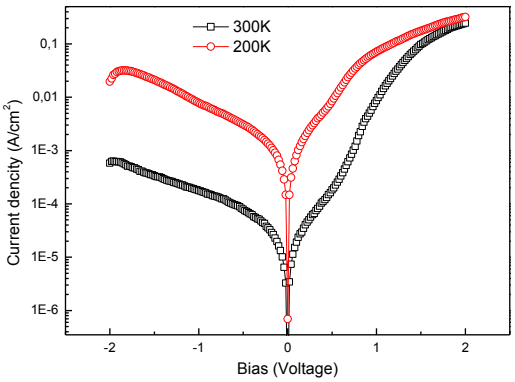

Fig. 8. Semilogarithmic current-voltage curve of Ag/n-ZnO/ Schottky diode.

The current density voltage graph of the Ag/ZnO diode fabricated with the cold substrate physical evaporation technique on the ZnO structures produced by the sol-gel method is presented in Figure 7. As can be seen, the contact created at the temperature of 200K shows a weak diode effect compared to the contact created at the temperature of 300K. The nanoparticle structure of the contacts formed at 200K may cause this situation. The reduction in particle size results in an increase in surface area and increased grain boundary interactions. This causes an increase in material resistance. While the diode produced at 200K is active at approximately ~ 0.5 volts, this cut-off voltage is approximately 1.0 volt for the diode produced at 300K. Although there is no early breaking under reverse bias, it is concluded that the diode obtained at 300K temperature is more stable.

The semi-logarithmic J-V characteristic of the created Schottky junction structure is given in Figure 8 and it can be said that the structure has a rectifying feature. The Ag/ZnO Schottky junction created at 200K shows diode behavior but approaches the ohmic feature. A similar situation was observed in Schottky Au/ZnO contacts produced by the Sol-gel technique [25]. Saturation current of Schottky diodes at room temperature is obtained from the extrapolation of the reverse current region of the logarithmic J-V graph. The reverse saturation current density is expressed as a function of the applied voltage (V) as follows [26];

$$I = I_0\left(e^{qV/nkT} - 1\right) \tag{7}$$

where I_0, q, V, k, n and T are saturation current, electronic charge, applied voltage, Boltzmann's constant, ideality factor, and temperature in Kelvin. The reverse saturation current I_0 is written by;

$$I_0 = AA^*T^2 e^{q\phi_{b0}/kT} \tag{8}$$

where A^* is the theoretical Richardson constant (32 A/cm^{2}K^2 for ZnO), A is the diode area and Φ_{bo} is the zero bias barrier height. From the slope of the straight-line region of the forward bias of ln(I)–V plot, the ideality factor (n) can be figured out and can be arranged as;

$$n = \frac{q}{kT}\frac{dV}{d(\ln I)} \tag{9}$$

The ideality factor is desired to be 1 ideally. But the ideality factor can take a value of 1 <n. If n is a value between 1 and 2, then the Tunneling Current Mechanism means dominant. If n = 2, the Generation-recombination Current Mechanism is dominant. It is concluded that the Leakage Current Mechanism is dominant, If n> 2 [14]. I_0 can be determined by extrapolating the forward bias of ln(I)–V curve to V = 0. The I-V curve reveals a low leakage current under reverse bias for the Schottky diode. Φ_{bo} can be obtained by the giving formula;

$$\phi_{b0} = \frac{kT}{q}\ln\left(\frac{AA^*T^2}{I_0}\right) \tag{10}$$

The experimental values of n, I_0 and Φ_{bo} with the help of given equations were given in Table 1.

Table 1. The characteristic Schottky diode values such as Ideality factor (n), Barrier height (Φ_{b0}), Series resistance (Rs) and saturation current (I_0) of Ag/ZnO device plotted and calculated from different graphs.

Device ZnO/Ag	V vs- log(I)			H(I) vs- I		dV/dln(I) vs I	
	n	I_0 (A)	Φ_{b0}(eV)	Φ_{b0} (eV)	Rs (Ω)	n	Rs (Ω)
200 K	15.6	4.7×10^{-4}	0.48	0.43	4.46	15.6	4.88
300 K	8.6	4.6×10^{-7}	0.66	0.15	3.65	7.41	4.78

The ideality factor was calculated to be 15.6 at 200K and 8.6-7.41 at 300K contact temperature from two different calculation methods. The ideality factor at 200K and 300K contact temperature exhibits a non-ideal diode characterization due to the homogeneity of the interface structure. High ideality factors can be attributed to the fact that the ideality factors calculated for the linear part of high voltage area. The theoretical model based on the Shah-Li-Schubert Theory is appropriate to clarify the anomalously high ideality factors [27]. In addition, Anomalously higher ideality factor at 200K then at 300K can be caused by the activation energies of the Ag atoms hitting the cold substrate surface as a result of physical evaporation are minimized and freezing on the surface, resulting in a homogeneous but amorphous surface contact layer. Ag atoms froze on the cold surface so the diffusion of them inside to the ZnO is decreased and a smoother surface is formed. This situation is supported by SEM images. Thus, this makes it possible to contact thin layers. These changes in the crystal structure of the Ag layer also affect the value of its work-function [28]. Perhaps, under normal conditions because of the work-function or/and thinness of the film, the Ag contact which will make ohmic contact with ZnO films, unlike obtained the Schottky contact structure. This can be supported to the number of working diodes on

a 1cm x 1 cm samples with the 1.5 mm^2 diode area. Although 15 out of 20 diodes in total at 200K contact temperature are working, this number has decreased to 5 in diodes obtained at 300K contact temperature. The barrier height is found as 0.48 and 0.43 eV at 200K and 0.66 and 0.15 eV at 300K contact temperature is almost close to the difference between the work functions of Ag (4.3 eV for polycrystals, 4.6-4.8 eV for single crystals with (100) plane index) [28] and n-ZnO (4.65 eV) [29]. The series resistance effect is one of the most significant reasons that deteriorating the ideal diode rectifying behavior. The current–voltage equation dependence of series resistance (R_s) is given by [26];

$$I = I_0[e^{q(V-IR_S)/nkT} - 1] \tag{11}$$

Φ_{bo}, n and R_s values of electrical parameters can also be measured and calculated from Cheung and Cheung proposed method [26]. Cheung and Cheung's functions can be calculated to determine the series resistance. Equation (11) can rearrange as follows;

$$\frac{dV}{d(\ln I)} = IR_S + \frac{nkT}{q} \tag{12}$$

According to Equation (12), the series resistance can be found from the slope and ideality factor is obtained by extrapolating the linear part of $dV/d(\ln I)$ versus I curve. If n = 1, the Equation (11) can be given as,

$$H(I) = IR_S + \frac{\phi_{b0}}{q} \tag{13}$$

where,

$$H(I) = V - \frac{kT}{q}\ln\left(\frac{I}{AA^*T^2}\right) \tag{14}$$

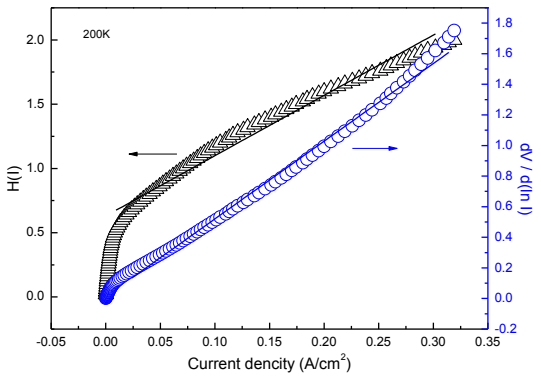

Fig. 9. dV/d(ln I) and H(I) versus I plot for calculating the values of ideality factor, series resistance, and barrier height for Ag/ZnO Schottky diode contacted under 200K substrate temperature.

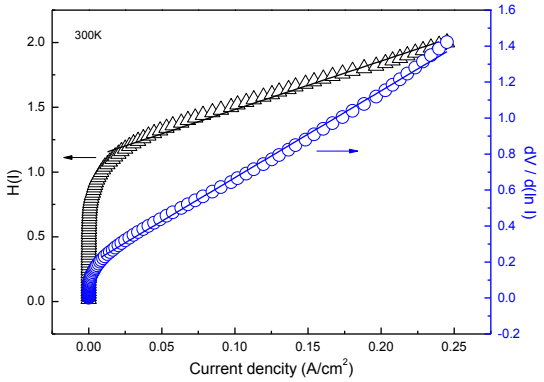

Fig. 10. dV/d(ln I) and H(I) versus I plot for calculating the values of ideality factor, series resistance, and barrier height for Ag/ZnO Schottky diode contacted under 300K substrate temperature.

Figures 9 and 10 show the *dV/d(ln I)* - *I* and *H(I)* - *I* graphs of Ag/ZnO Schottky diodes obtained at 200K and 300K temperatures, respectively. A second determination of the series resistance (R_s) and the barrier height (Φ_{bo}) can be calculated from the slope of the straight-line region of *H*(*I*)–*I* graph and intercept of the *H*(*I*) axis versus $I = 0$, respectively. The results calculated I_0, Φ_{b0}, *Rs* values are presented in Table 1. The ideality factor was obtained at high values due to the very thin ZnO films (~ 300nm). Here, the current mechanism consists of the accumulation of charge carriers. Yakuphanoglu et al. [17] has determined ideality factor with high values similarly.

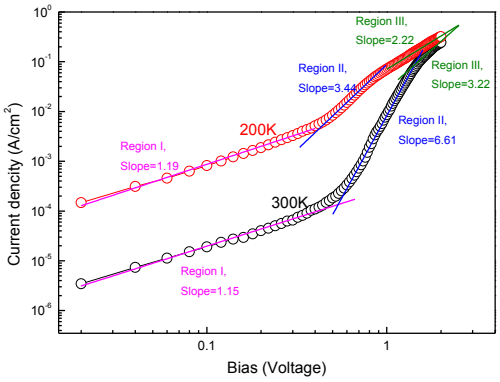

Fig. 11. The current-voltage (I–V) characteristic in a double logarithmic plot for the Ag/n-ZnO diode at 200K and 300K contact temperatures.

The double logarithmic *I–V* plot for the Ag/ZnO/SnO_2 structure has been presented in Figure 11. It can be attributed to the difference of slope, the forward bias characteristic of the Ag/ZnO/SnO_2 junction structure has three distinct linear regions. This situation reports that there are varied transportation mechanisms for the hetero-structure with the slope value of 1.15, 6.61 and 3.22 for the region I, II and III for 300K and slope value of 1.19, 3.44 and 2.22 for 200K contact temperature, respectively. In region II and III, the slope of I-V has been obtained as the value larger than 2.0 that attributes the possibility of the space-charge-limited-current mechanism (SCLC) according to Mott-Gurney law ($J \sim V^2/d^3$) [30, 31]. At low voltages there is no ohmic characteristic in contrast to classically which can be caused by the depletion layer with an electron confinement well structure (about 300 nm thickness) between Ag and n-ZnO Schottky device on SnO_2 of. In region II, the slope of double logarithmic I-V is increased that means can be the mobility of charge carriers increased with raising the applied voltage. In region III, at the high voltages, the slope tends to decrease because the complex device approaches the 'trap-filled' limit

when the injection level is high whose dependence is the same as in the Trap-free Space-charge-limited current [14, 32, 33].

4. Conclusion

We carried out a detailed characterization of ZnO thin films on glass and SnO_2 substrate and fabrication of Ag/n-ZnO/SnO2/Glass architecture for Schottky diode by Sol-gel spin coating and Cold Substrate physical vapor deposition technique for coating and contacting. Devices such as diode, hetero/homo-structure on the n-type property of ZnO crystals have become an important component for sensor application or catalyst the toxic gas. Ag metal electrode is applied onto n-ZnO at 200K and 300K substrate temperatures, and electricity is generated due to the Schottky barrier formed between ZnO and Ag. Herein, a rectifying diode is obtained with a high n value of 15.6 at 200K and 8.6-7.4 at 300K contact temperature according to dV/dln(I) vs I and H(I) versus I. The electrons trapped in a ZnO energy well between Ag and SnO_2 layers with 300 nm average thickness.

The film shows up hexagonal wurtzite structure with a strong (002) preferred direction perpendicular to the substrate. Ideality factor of the Ag/n-ZnO diode is anomalously high (n >2), which indicates that the Leakage Current Mechanism is dominant and principal theory of conduction mechanism for current flow. As a result, 15 of the diodes produced in 200K showed diode characteristics, whereas this number is only 5 diodes for 300K contact temperature. This is a very significant result for solving a problem about chip fabrication which has billion of semiconductor devices on it.

References

[1] L .C. Klein, Solid State Ionics **26**, 143 (1988).
[2] W. Zhang, J. J. Li, P. Guan, C. X. Lv, C. Yang, N. Han, X. C. Wang, G. J. Song, Z. Peng, J Alloy Compd, 835 (2020).
[3] M. E. Ganji, A. M. Bazargan, M. Keyanpour-Rad, M. A. Bahrevar, Funct Mater Lett **3**, 141 (2010).
[4] J. L. Ning, D. M. Jiang, K. B. Shim, Adv Appl Ceram **105**, 265 (2006).
[5] H. K. Verma, D. Rehani, S. N. Sharma, K. K. Maurya, Optik, 204 (2020).
[6] B. Fanady, W. Song, R. X. Peng, T. Wu, Z. Y. Ge, Org Electron, 76 (2020).
[7] U. Ozgur, Y. I. Alivov, C. Liu, A. Teke, M. A. Reshchikov, S. Dogan, V. Avrutin, S. J. Cho, H. Morkoc, J Appl Phys, 98 (2005).
[8] L. E. Aygun, P. Kumar, Z. W. Zheng, T. S. Chen, S. Wagner, J. C. Sturm, N. Verma, Ieee T Biomed Circ S **13**, 1264 (2019).
[9] Z. S. Chen, Z. Chen, Z. L. Song, W. H. Ye, Z. Y. Fan, J Semicond, 40 (2019).
[10] S. Ali, S. Saleem, M. Salman, M. Khan, Mater Chem Phys, 248 (2020).
[11] Z. N. Kayani, Z. Bashir, S. Riaz, S. Naseem, Z. Saddiqe, Mater Sci-Mater El, (2020).
[12] A. C. Garcia-Velasco, A. Baez-Rodriguez, M. Bizarro, L. Garcia-Gonzalez, J. Hernandez-Torres, L. Zamora-Peredo, Nanotechnology, 31 (2020).
[13] V. Nevruzoglu, D. B. Altuntas, M. Tomakin, Appl Phys a-Mater, 126 (2020).
[14] E. F. Keskenler, M. Tomakin, S. Dogan, G. Turgut, S. Aydin, S. Duman, B. Gurbulak, J Alloy Compd **550**, 129 (2013).
[15] G. M. Ali, M. A. Hashem, M. W. Naji, 2015 Third International Conference on Technological Advances in Electrical, Electronics and Computer Engineering (Taeece), 212 (2015).
[16] N. Guy, M. Ozacar, Int J Hydrogen Energ **41**, 20100 (2016).
[17] S. A. Mansour, F. Yakuphanoglu, Solid State Sci **14**, 121 (2012).
[18] J. K. Rajput, T. K. Pathak, V. Kumar, H. C. Swart, L. P. Purohit, Rsc Adv **9**, 31316 (2019).
[19] E. F. Keskenler, S. Dogan, G. Turgut, B. Gurbulak, Metall Mater Trans A **43a**, 5088 (2012).
[20] G. Anoop, K. M. Krishna, K. R. Kumar, M. K. Jayaraj, J Electrochem Soc **155**, J270 (2008).

[21] S. H. Mousavi, T. S. Muller, P. W. de Oliveira, J Mater Sci-Mater El **24**, 3338 (2013).
[22] S. Thongma, K. Tantisantisom, N. Grisdanurak, T. Boonkoom, Sensor Actuat a-Phys **296**, 324 (2019).
[23] T. Torchynska, B. P. Millan, G. Polupan, M. Kakazey, J Electron Mater **47**, 4296 (2018).
[24] T. V. Torchynska, B. El Filali, J Lumin **149**, 54 (2014).
[25] J. D. Hwang, C. Y. Kung, Y. L. Lin, Ieee T Nanotechnol **12**, 35 (2013).
[26] S. K. Cheung, N. W. Cheung, Appl Phys Lett **49**, 85 (1986).
[27] C.-X. Wang, G.-W. Yang, H.-W. Liu, Y.-H. Han, J.-F. Luo, C.-X. Gao, G.-T. Zou, Appl Phys Lett **84**, 2427 (2004).
[28] V. Likholobov, P. Simonov, Physicochemical Aspects of Preparation of Carbon-Supported Noble Metal Catalysts, (2003).
[29] V. Quemener, M. Alnes, L. Vines, P. Rauwel, O. Nilsen, H. Fjellvag, E. V. Monakhov, B. G. Svensson, J Phys D Appl Phys, 45 (2012).
[30] S. Aydogan, M. Saglam, A. Turut, J Phys-Condens Mat **18**, 2665 (2006).
[31] L. Pauling, The Journal of Physical Chemistry **45**, 1142 (1941).
[32] O. Gullu, S. Aydogan, A. Turut, Microelectron Eng **85**, 1647 (2008).
[33] P. N. Murgatroyd, Journal of Physics D: Applied Physics **3**, 151 (1970).